Structure-based Virtual Screening to Get New Scaffold Inhibitors of the PknB from Mycobacterium tuberculosis

Short Communication

Antonio Coluccia[1], Giuseppe La Regina[1], Nathalie Barilone[2], María-Natalia Lisa[2], Andrea Brancale[3], Gwenaëlle André-Leroux[2,4], Pedro M. Alzari,[2] and Romano Silvestri[1]

[1] Istituto Pasteur – Fondazione Cenci Bolognetti, Dipartimento di Chimica e Tecnologie del Farmaco, Sapienza Università di Roma, Piazzale Aldo Moro 5, I-00185 Roma, Italy
[2] Institut Pasteur, Unité de Microbiologie Structurale, CNRS UMR3528, 25 Rue du Dr. Roux, F-75724 Paris, France
[3] Welsh School of Pharmacy, Cardiff University, King Edward VII Avenue, Cardiff, CF10 3NB, UK
[4] Inra, Unité Mathématique, Informatique & Génome, Domaine de Vilvert, 78352 Jouy-en-Josas Cedex, France

Corresponding author: Prof. Romano Silvestri, Dipartimento di Chimica e Tecnologie del Farmaco, Sapienza Università di Roma, Piazzale Aldo Moro 5, I-00185 Roma, Italy
E-mail: romano.silvestri@uniroma1.it
Phone: +39 06 4991 3800
Fax: +39 06 4991 3993

Additional supporting information may be found in the online version of this article at the publisher's web-site.

Summary. In search of new inhibitors of the Ser/Thr protein kinase PknB from Mycobacterium tuberculosis we carried out a structure-based virtual screening study to identify ATP-competitive inhibitors of this enzyme. These studies resulted in the identification of N-phenylmethylindole-2-carboxamide as a promising scaffold for the development of new PknB inhibitors. We synthesized a small set of compounds to assess the pharmacophore structural requirements and to optimize the inhibitory activity against PknB. This strategy led to the identification of compound 3, endowed with an IC_{50} of 20 μM, which provides a novel scaffold for further improvement of PknB inhibitors.

Introduction

Mycobacterium tuberculosis (Mtb) is the etiological agent of tuberculosis (TB), a major infectious disease that affects millions of people every year. As a bacterial pathogen, Mtb is the second leading cause of death, after the human immuno- deficiency virus [1]. The rapid emergence of first- and second-line drug resistant Mtb strains highlights the urgent need for new drugs to treat TB.

Mtb has a complex and dynamic life cycle including replicative and dormant states, highlighting that Mtb bacilli possess efficient signaling systems to sense the surroundings and adapt the physiology accordingly. Mtb codes for eleven eukaryotic-like Ser/Thr Protein Kinases (STPKs) [2]. Among these, the trans-membrane (receptor-like) STPK PknB is the only Mtb kinase that is upregulated during the exponential growth phase [3-5] upon macrophage infection [6] and repressed under nutrient starvation in a model of persistent Mtb [7]. Furthermore, PknB has been shown to be essential for Mtb growth [8] being required to phosphorylate substrates involved in cell-wall biogenesis [9]. Therefore, PknB has been established as a valid target for the design of new anti TB drugs [10-12].

The PknB kinase domain adopts the typical two-lobed structure found in STPKs. The kinase N-lobe encompasses several β-sheets and a regulatory α-C helix, while the C-terminal lobe is mainly helical. The ATP-binding and protein substrate-binding sites reside at the interface between these two sub-domains [13,14].
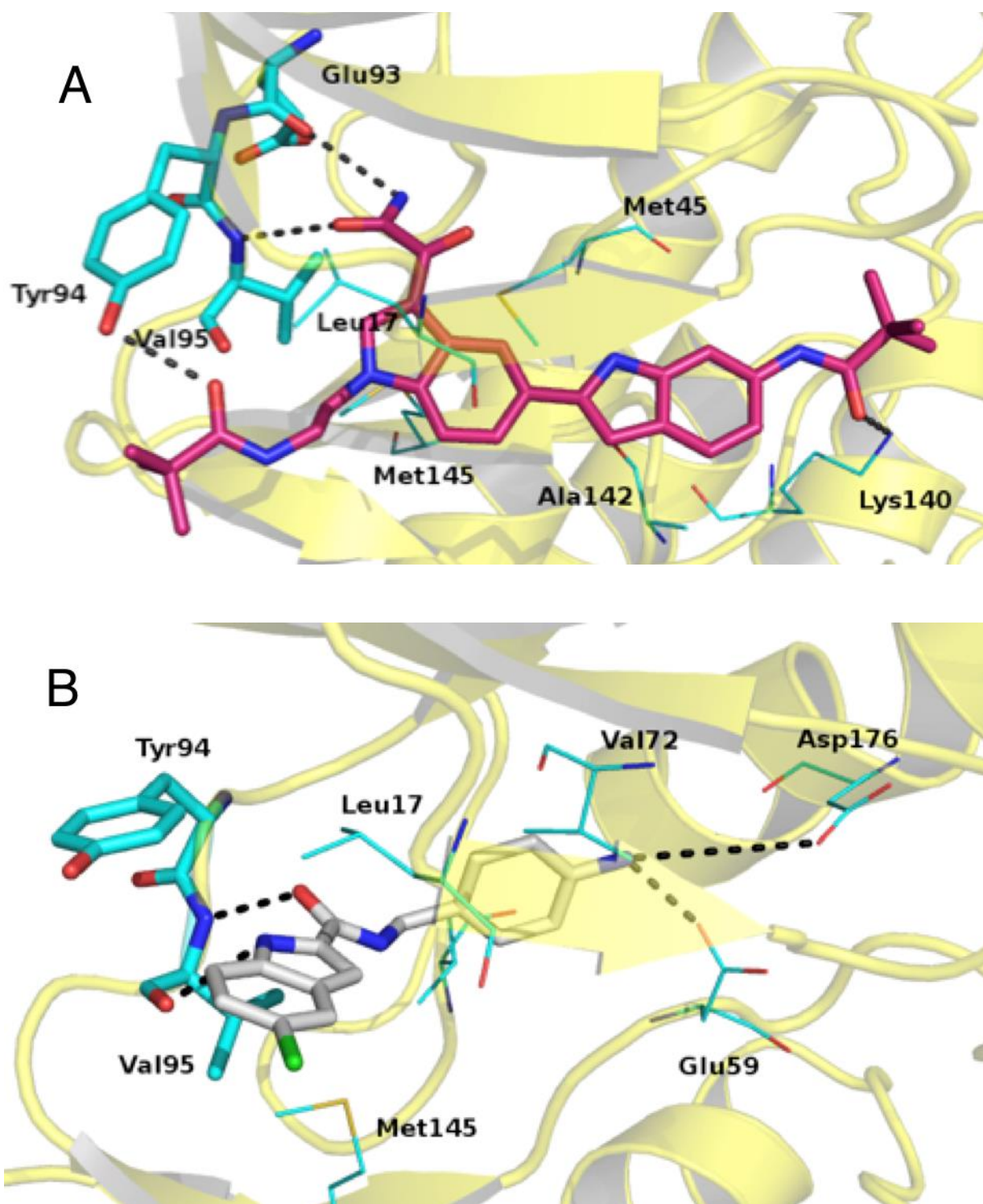
Figure 1. Binding mode of 1 (magenta) (panel A) and 2 (gray) (panel A) proposed by Plants. Residues involved in interactions are highlighted as lines, hinge region residues are reported as stick (cyan), the PknB ATP binding site is shown as a cartoon (yellow) and H-bonds are depicted as dotted lines (black).

Results and discussion

Virtual screening study

We carried out a structure-based virtual screening (VS) study using an in-house library of 5000 compounds, all following Lipinski's rules [15], and the crystal structure of PknB obtained in presence of the competitive inhibitor mitoxantrone (PDB code: 2FUM) [16]. The whole compound library was docked into the PknB ATP binding site using Plants [17] and Autodock [18]. To assess the ability of the docking protocol to discriminate active vs inactive compounds, we separately analysed a test set comprising the co-crystallized mitoxantrone and other PknB inhibitors previously studied [12]. Both Plants and Autodock provided consistent binding modes for all compounds, but the correlation between docking score and in vitro inhibitory activity was unsatisfactory. Hence, we decided to select only those compounds having a RMSD <2, between the best energy poses obtained by Plants and Autodock [19]. This selection filtered the library including over 1000 compounds, which were then ranked by number of H-bonds formed with the hinge region of PknB [20]. The best 100 molecules were visually inspected and the most promising molecules were experimentally analysed to assess their in vitro inhibitory activity against PknB. Compounds **1** and **2** were newly synthesized and evaluated as PknB inhibitors. These compounds inhibited 50% of PknB kinase activity at the concentration of 100 μM (Table 1).

Compound **1** was predicted to bind the ATP pocket of PknB by establishing two H-bonds with residues Glu93 and Val95 in the kinase hinge region, which acts in the positioning of the ATP substrate. The bis-indole moiety is stabilized by hydrophobic interactions with the side chains of residues Leu17 (at the N-terminus of the kinase glycine rich loop), Met45, Ala142 and Met145 (deep in the ATP binding pocket). An additional key H-bond engages residue Lys140, located in the catalytic loop of PknG, right after the HRD motif (Figure 1A).

Compound **2** also binds the ATP pocket of PknB by forming H-bonds with the kinase hinge region. While the compound indole ring establishes hydrophobic interactions with residues Leu17 and Met145, the benzyl ring interacts with the side chains of Val25 and Val72. Also, the aromatic amino group establishes two H-bonds, one with the conserved residue Glu59 (involved in the locked-in positioning of the regulatory αC helix through a salt bridge with the catalytic Lys40), and other with residue Asp176 in the DFG motif (Figure 1B).

Table 1. Structure and PknB Inhibition by Compounds 1-9[a)]
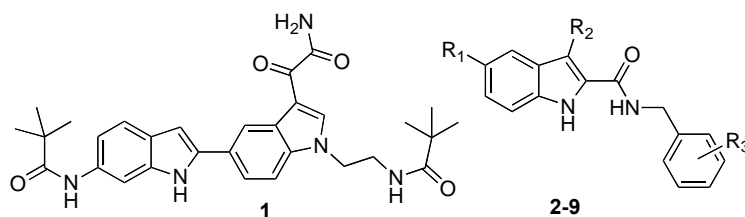
Compound	R$_1$	R$_2$	R$_3$	PknB % inhibition[b)]
1	-	-	-	50
2	Cl	H	4-NH$_2$	50
3	Cl	Phenyl	3-NH$_2$	83
4	Cl	H	3-Cl	42
5	Cl	H	3-NH$_2$	20
6	Br	H	3-NH$_2$	20
7	Cl	H	4-NO$_2$	56
8	Cl	H	2-NH$_2$	39
9	Cl	H	2-NO$_2$	53

[a)] Data are mean values of two to three independent experiments performed in duplicate. Standard deviations correspond to 10% of the measured value in each case.
[b)] PknB % of inhibition; PknB was 30 nM, GarA was 20 μM and compound was 100 μM.

While compounds **1** and **2** were determined to be equipotent as PknB inhibitors, **2** was selected for further optimization because of its better drug-like properties predicted by QikProp software [21]. Descriptors computed for compound **2** were always better than that of compound **1** (Table 1S Supporting Information). Indeed no deviation from Lipinski's rule was accounted.

Molecular dynamics (MD) simulations of the PknB-**2** complex confirmed the H-bonds between the compound and the residues within the kinase hinge region, with a calculated rate of formation <80%. The hydrophobic contacts remained stable along the trajectory, while the H-bonds involving the compound aromatic amino group disappeared quickly. No significant movements of the complex were observed, suggesting the stabilization of the two kinase lobes upon ligand binding (Figure 1S, Supporting Information).

An in-silico library of compound **2** analogues was generated by superimposition of its binding mode with those of compounds within the test set. Compounds **3-9** (Table 1),

which were predicted as the most efficient PknB inhibitors by docking simulations, were synthesized and analyzed in vitro.

It is well known that many kinase inhibitors are not selective because they interact with the ATP binding region that has similar geometry amongst the protein kinases. With the aim of assessing the compounds selectivity we firstly identified the kinases (available at protein data bank [22]) with the highest PknB similarity score, using CPASS [23, 24]. We then docked compounds **2-9** with the proteins identified in the previous step. CPASS identified three other kinases as the most similar to PknB: MAP1 (64.1%), GSK-3β (□□□3%) and Aurora-A (60.8%). Compounds **2-9** binding poses for MAP1 and GSK-3β □□□□□□□□□□□□□□□□□ with these observed for PknB, while a different binding mode was observed for Aurora-A. From these results we could speculate that the compounds reported might not be very selective toward PknB, following the definition of kinase type I inhibitors [25].


Chemistry

Synthesis of **1** was carried out by a Pd-mediated cross-coupling reaction **13** and **24** (Scheme 1). Carboxamides **4**, **17** and **18** were synthesized by coupling the indole-2-carboxylic acid **14-16** with the corresponding amine in the presence of BOP reagent and triethylamine (TEA) in anhydrous DMF at 25 °C for 12 h (Scheme 2). Alternatively, an appropriate carboxylic acid was activated by treatment with 1,1'-carbonyldiimidazole in anhydrous THF, then treated with the amine to produce compounds **9** or **19**. Compound **7** was obtained by reaction of **15** with 4-nitrobenzylamine hydrochloride in the presence of PyBOP reagent and TEA in anhydrous DMF at 25 °C for 12 h. Tin(II) chloride reduction of the nitro derivatives **7**, **9** and **17-19** in ethyl acetate at 80 °C for 3 h furnished compounds **2**, **3**, **5**, **6** and **8**, respectively. Pinacol ester **13** was synthesized starting from **10** that, after reaction with pivaloyl chloride in the presence of TEA in anhydrous THF at 25 °C for 12 h, was iodinated at position 2 by using the Katritzky method [26] and then transformed into the corresponding boronic ester according to Miyaura reaction conditions [27] under microwave (MW) irradiation (Scheme 1). Reaction of **20** with chloroacetonitrile in the presence of NaH in anhydrous DMF at 25 °C for 12 h furnished derivative **21**, that after reduction with LiAlH₄ in anhydrous THF at 50 °C for 4 h and subsequent treatment with pivaloyl chloride, as above described, was transformed into **22** (Scheme 3). Compound **22**

was treated with oxalyl chloride in anhydrous diethyl ether for 3 h and then with methanol in the presence of TEA for 5 h to furnish the methyl 2-oxoacetate **23**, that was converted into the corresponding amide **24** by treatment with 28% NH4OH in ethanol at 130 °C (150 W) for 15 min. Carboxylic acid **14** was obtained by bromination of ester **25** with N-bromosuccinimide (NBS) to give the corresponding 3-bromo derivative **26** (Scheme 4). Treatment of **26** with phenylboronic acid in the presence of Pd(dppf)Cl2·CH2Cl2 and Na2CO3 in 1,4-dioxane at 100 °C for 16 h provided the 3-phenylindole **27** (Scheme 4). Compound **27** was transformed into the corresponding carboxylic acid **14** by hydrolysis with LiOH·H2O in aqueous THF at 25 °C for 12 h.
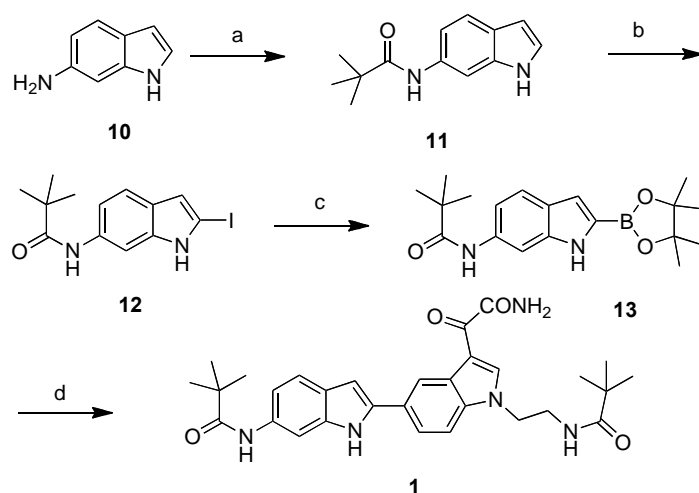
Scheme 1. Chemical synthesis of compound **1**. Reagents and conditions: (a) pivaloyl chloride, TEA, anhydrous THF, 25 °C, 12 h, 82%; (b) (i) n-BuLi, -78 °C, anhydrous THF, Ar stream, 30 min; (ii) CO2g, 10 min; (iii) tert-BuLi, -78 °C, anhydrous THF, Ar stream, 1 h; (iv) 1,2-diiodoethane, -78 °C, 1 h, Ar stream, 25%; (c) pinacol borane, TEA, SPhos, PdCl2(CH3CN)2, toluene, closed vessel, 250 W, 20 min, PowerMAX, 97%; (d) 24, K3PO4, DMF, Pd(dppf)Cl2·CH2Cl2, 60 °C, 1 h, Ar stream, 85%.
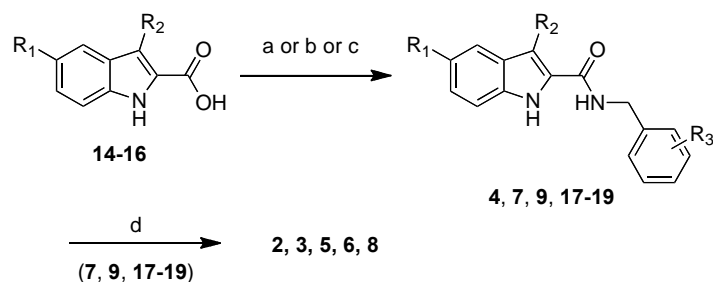
Scheme 2. Chemical synthesis of compounds **2-9** (Table 1); **14**: R_1 = Cl, R_2 = Ph; **15**: R_1 = Cl, R_2 = H; **16**: R_1 = Br, R_2 = H; **17**: R_1 = Cl, R_2 = H, R_3 = 3-NO$_2$; **18**: R_1 = Br, R_2 = H, R_3 = 3-NO$_2$; **19**: R_1 = Cl, R^2 = Ph, R_3 = 3-NO$_2$. Reagents and conditions: (a) (**4**, **10**, **11**) amine, BOP reagent, TEA, anhydrous DMF, 25 °C, 12 h, 47-81%; (b) (**9**, **12**) (i) 1,1'-carbonyldiimidazole, anhydrous THF, 25 °C, 2 h; (ii) amine, 25 °C, 2 h, 42-59%; (c) (**7**) amine, PyBOP reagent, TEA, anhydrous DMF, 25 °C, 12 h, 30%; (d) SnCl$_2$·2HO, AcOEt, 80 °C, 3 h, 54-87% .
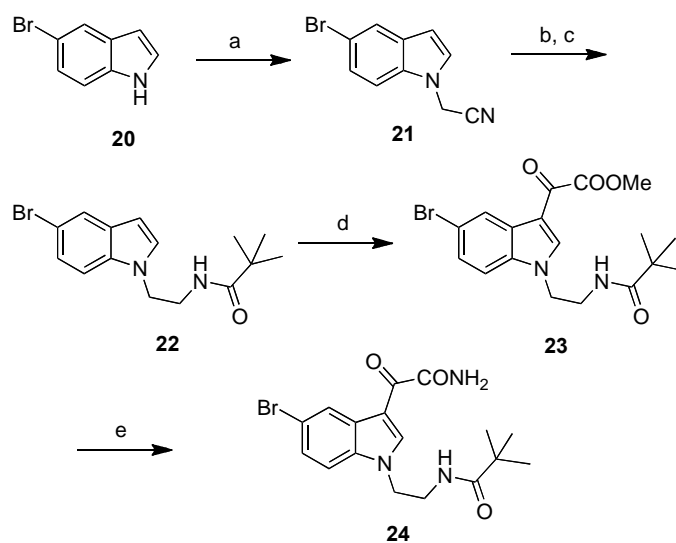
Scheme 3. Chemical synthesis of compound **24**. Reagents and conditions: (a) (i) NaH, anhydrous DMF, 25 °C, 30 min; (ii) chloroacetonitrile, 25 °C, 12 h, 40%; (b) LiAlH$_4$, anhydrous THF, 50 °C, 4 h, crude product; (c) pivaloyl chloride, TEA, anhydrous THF, 50 °C, 12 h, 10%; (d) (i) oxalyl chloride, anhydrous Et$_2$O, 0 °C for 1.5 h then 25 °C for 1.5 h, Ar stream; (ii) MeOH, TEA, 0 °C for 1 h then 25 °C for 4 h, 25%; (e) 28% NH$_4$OH, EtOH, closed vessel, 150 W, 130 °C, 15 min, 73%.
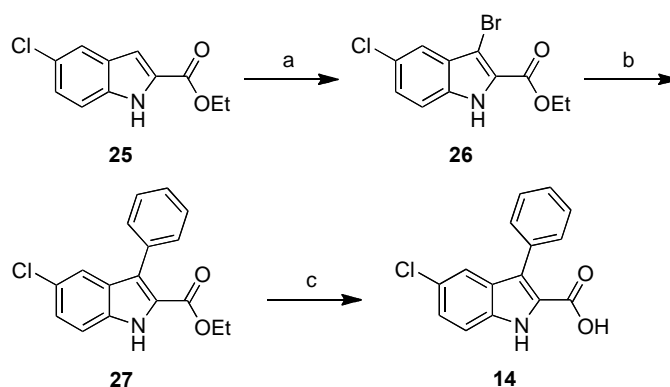
Scheme 4. Chemical synthesis of compound **14**. Reagents and conditions: (a) NBS, anhydrous DMF, 80 °C, 3 h, 37%; (b) phenylboronic acid, Pd(dppf)Cl$_2$·CH$_2$Cl$_2$, Na$_2$CO$_3$, 1,4-dioxane, 100 °C, 16 h, 70%; (c) LiOH·H$_2$O, THF/H$_2$O, 25 °C, 12 h, 96%.

Biological activity

Among the group of compounds **3-9**, bearing the N-benzyl at the indole-2-carboxamide, derivative **3** inhibited PknB activity by 83% at a concentration of 100 µM and showed an IC$_{50}$ value of 20 µM. There was no evident major difference among the substituents at the N-benzyl moiety of **4-9**. These compounds inhibited PknB in the 39-56% range, although the data are limited. Docking analyses of **3** showed the 3-phenyl ring filled a hydrophobic pocket comprising residues Leu17 and Met155, thus ensuring a better stabilization of the complex within PknB active site (Figure 2). MD simulations of the complex PknB-**3** highlighted a rate of formation near to 100% for the H-bonds within the kinase hinge region, evidencing an improvement over compound **2**. The 3-phenylindole group established contacts with PknB residues Met145, Met155 and Leu17. The benzyl ring was stabilized by hydrophobic contacts with Val25, no H-bond interactions were observed for the 3-amino group.
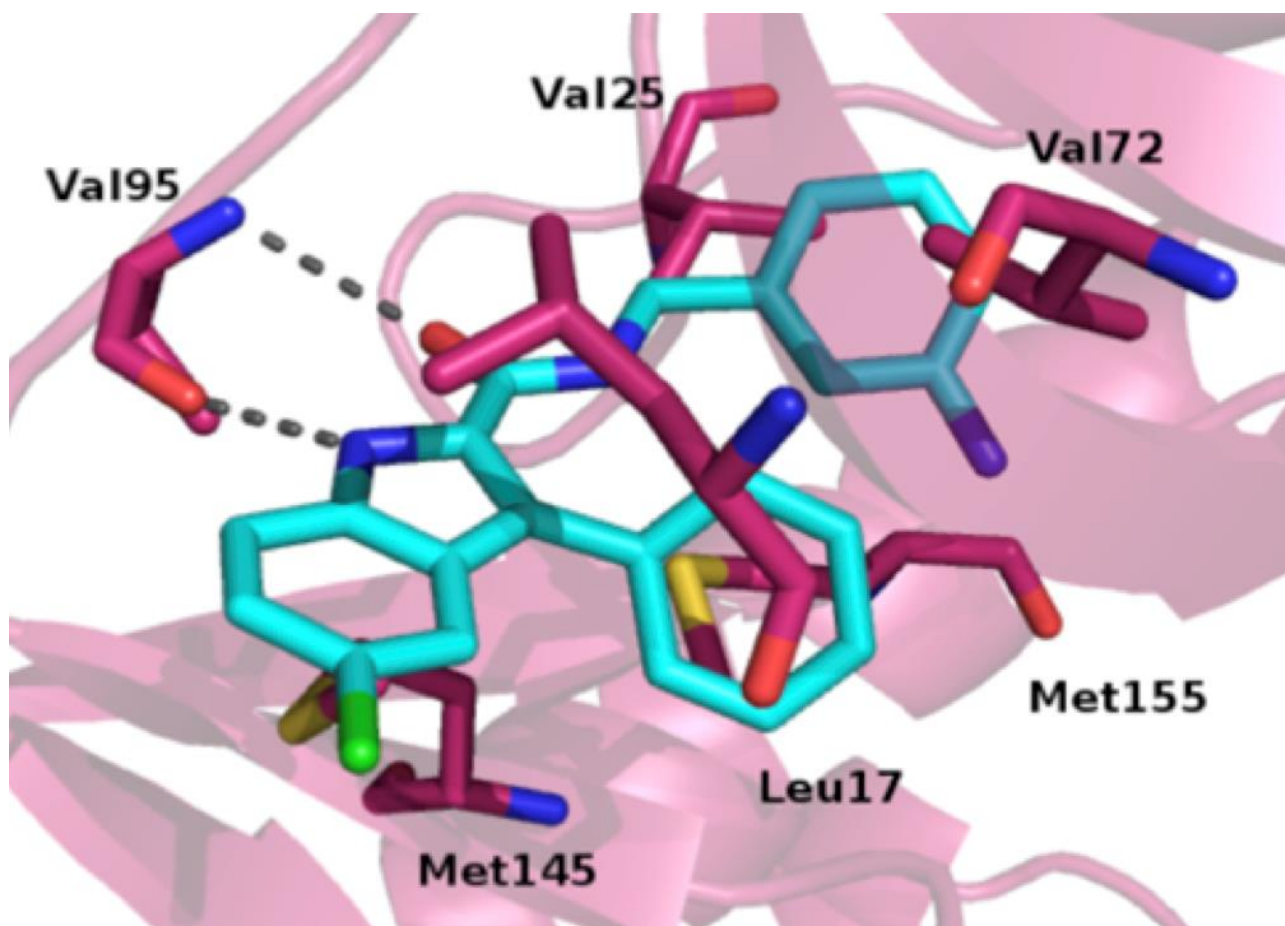
Figure 2. Snapshot of compound 3 (cyan) trajectory. Residues involved in interactions are depicted as sticks (magenta), the PknB binding site is shown as a cartoon and H-bonds are depicted as dotted lines (black).

Conclusion

A structure-based VS using the ATP binding site of the Ser/Thr protein kinase PknB was a powerful technique for the discovery of novel scaffolds **1** and **2** with PknB inhibitory activity. Additional in silico studies led to design and synthesize a small compound library of compounds **3-9**. Compound **3** showed promising inhibition with activity an IC_{50} value against PknB of 20 μM. Current investigations are progress in our research group to clarify the structural requirements for further development of this novel class of potential anti-Mtb compounds.

Experimental

Chemistry

*N-(3'-(2-Amino-2-oxoacetyl)-1'-(2-pivalamidoethyl)-1H,1'H-[2,5'-bi-indol]-6-yl)pivalamide (**1**).*
A mixture of **13** (0.34 g, 0.99 mmol), **24** (0.30 g, 7.6 mmol) and K_3PO_4 (0.48 g, 2.3 mmol) in DMF was degassed for 15 min. Pd(dppf)Cl_2·CH_2Cl_2 (0.019 g, 0.023 mmol) was added and the reaction mixture was heated at 60 °C for 1 h under Ar stream, cooled and diluted with water. The organic layer was extracted with ethyl acetate, washed with brine, dried and filtered. Removal of the solvent gave a residue that was purified by column chromatography (silica gel, ethyl acetate:ethanol = 95:5 as eluent) to furnish **1** (0.34 g, 85%), mp 165-168 °C (from ethanol). ^1H NMR (DMSO-d_6): δ 0.96-1.00 (m, 9H), 1.22-1.26 (m, 9H), 3.41-3.45 (m, 2H), 4.39-4.41 (m, 2H), 6.75-6.77 (m, 1H), 7.13-7.16 (m, 1H), 7.39-7.80 (m, 4H; 2H after treatment with D_2O), 7.92-7.94 (m, 1H), 8.05 (br s, disappeared on treatment with D_2O, 1H), 8.34-8.36 (m, 1H), 8.67-8.70 (m, 2H), 9.07-9.09 (m, disappeared on treatment with D_2O, 1H), 11.52 ppm (br s, disappeared on treatment with D_2O, 1H). IR: ν 1625, 2961, 3318 cm^{-1}. Anal. calcd for $C_{30}H_{35}N_5O_4$ (529.64); calcd %: C 68.03, H 6.66, N 13.22, found %: C 68.00, H 6.61, N 13.20.

*General procedure for the synthesis of compounds **2**, **3**, **5**, **6** and **8**. Example. N-(4-Aminobenzyl)-5-chloro-1H-indole-2-carboxamide (**2**).*
$SnCl_2$·$2H_2O$ (0.203 g, 0.9 mmol) was added to a solution of **7** (0.10 g, 0.3 mmol) in ethyl acetate (18.0 mL). The reaction was heated at reflux at 80 °C for 3 h. After cooling, the reaction mixture was made basic with a saturated aqueous solution of $NaHCO_3$ and filtered. The organic layer was washed with brine, dried and filtered. Removal of the solvent gave a residue that was purified by column chromatography (silica gel, n-hexane:ethyl acetate = 2:3 as eluent) to provide **2** (0.06 g, 66%), mp 236-240 °C (from ethanol). ^1H NMR (DMSO-d_6): δ 4.30-4.31 (d, J = 4.8 Hz, 2H), 4.96 (br s, disappeared on treatment with D_2O, 2H), 6.50-6.52 (d, J = 7.6 Hz, 2H), 6.97-6.99 (d, J = 8.0 Hz, 2H), 7.12 (s, 1H), 7.15-7.17 (d, J = 8.0 Hz, 1H), 7.40-7.42 (d, J = 8.4, 1H), 7.67 (s, 1H) , 8.91 (br s, disappeared on treatment with D_2O, 1H), 11.77 ppm (br s, disappeared on treatment with D_2O, 1H). IR: ν 1640, 3219, 3408, cm^{-1}. Anal. calcd for $C_{16}H_{14}ClN_3O$ (299.76); calcd %: C 64.11, H 4.71, N 14.02, Cl 11.83, found %: C 63.88, H 4.65, N 13.78, Cl 11.55.

N-(3-Aminobenzyl)-5-chloro-3-phenyl-1H-indole-2-carboxamide (3).

Was synthesized as **2** starting from **19**. Yield 54%, mp 145-150 *C (from ethanol). ^{1}H NMR (DMSO-d6): δ 4.23-4.24 (d, J = 5.8 Hz, 2H), 5.00 (br s, disappeared on treatment with D_2O, 2H), 6.31-6.33 (d, J = 7.16 Hz, 1H), 6.40-6.42 (m, 2H), 6.89-6.93 (t, J = 8.2 Hz, 1H), 7.22-7.26 (m, 1H), 7.32-7.36 (m, 1H), 7.42-7.49 (m, 6H), 7.80-7.82 (t, J = 6.1 Hz, disappeared on treatment with D_2O, 1H), 11.96 ppm (br s, disappeared on treatment with D_2O, 1H). IR: ν 1649, 3130, 3408 cm^{-1}. Anal. calcd for $C_{22}H_{18}ClN_3O$ (375.86); calcd %: C 70.30, H 4.83, N 11.18, Cl 9.43, found %: C 70.12, H 4.78, N 10.95, Cl 9.22.

Biological assays

PknB inhibition assay

PknB inhibition assays were carried out in a final volume of 20 μL, containing 50 mM HEPES, pH 7.0, 1 mM DTT, 1 mM $MnCl_2$ and 20 μM GarA as a substrate. Compounds (100 μM in each case) were initially incubated for 30 min at 4 °C with the reaction mixture containing 30 nM PknB. Then, kinase reactions were started by adding 100 μM ATP (1 μCi of [$\square$-^{33}P] ATP) and were carried out for 30 min at 37 °C. Reactions were stopped by heat inactivation for 4 min at 95 °C in the presence of SDS 2% w/v and 6 $\square$L were spotted onto P81 paper (phosphocellulose, Whatman). The paper was washed with 1% v/v phosphoric acid, rinsed with acetone and allowed to dry. Radiolabelled spots were analyzed with a phosphoimager (Storm, Molecular Dynamics). Each reaction was performed in duplicates [28].

Molecular modelling

Hydrogen atoms were added to the crystal structure of PknB (PDB code: 2FUM) by using Molecular Operating Environment (MOE) 2007.09 [29] and minimized, keeping all the heavy atoms fixed until a rmsd gradient of 0.05 kcal mol-1 Å^{-1} was reached. Ligand structures were built with MOE and minimized using the MMFF94x force field until a rmsd gradient of 0.05 kcal mol^{-1} Å^{-1} was reached. Docking simulations were performed using PLANTS [17] and Autodock 4.0 [19]. We set up the binding lattice on a sphere of 15 Å radius for PLANTS and on a cubic lattice of 60 60 60 npts for Autodock, centered on the inhibitor mitroxantone. Default settings were used.

Molecular dynamics were performed employing the AMBER 10 suite [30, 31] The minimized structure was solvated in a periodic octahedron simulation box, using TIP3P

water molecules, providing a minimum of 10 Å of water between the protein surface and any periodic box edge. Ions were added to neutralize the charge of the total system. The water molecules and Na^+ ions were energy-minimized, keeping the coordinates of the protein-ligand complex fixed (1,000 cycles), and then the whole system was minimized (5,000 cycles). Next, the entire system was heated and thermalized to 298 K (5 ps). The simulation was conducted at 298 K, with constant pressure and periodic boundary condition. Shake bond length condition was used (ntc = 2). Compounds were parameterized by Antechamber [32, 33] using BCC charges. Trajectories analysis were carried our by ptraj program [34]. The images in the manuscript were created with PyMOL [35].

## References

[1] Global Tuberculosis Report 2012, www.who.int/topics/tuberculosis/.

[2] S.T. Cole, R. Brosch, J. Parkhill, T. Garnier, C. Churcher, D. Harris, S. V. Gordon, K. Eiglmeier, S. Gas, C.E. Barry, III, F. Tekaia, K. Badcock, D. Basham, D. Brown, T. Chillingworth, R. Connor, R. Davies, K. Devlin, T. Feltwell, S. Gentles, N. Hamlin, S. Holroyd, T. Hornsby, K. Jagels, A. Krogh, J. McLean, S. Moule, L. Murphy, K. Oliver, J. Osborne, M.A. Quail, M.-A. Rajandream, J. Rogers, S. Rutter, K. Seeger, J. Skelton, R. Squares, S. Squares, J. E. Sulston, K. Taylor, S. Whitehead, B. G. Barrell. *Nature* **1998**, *393*, 537–544.

[3] Y. Av-Gay, S. Jamil, S.J. Drews. *Infect. Immun.* **1999**, *67*, 676–682.

[4] C.M. Sassetti, D.H. Boyd, E.J. Rubin. *Mol. Microbiol.* **2003**, *48*, 77–84.

[5] C.M. Kang, D.W. Abbott, S.T. Park, C.C. Dascher, L.C. Cantley, R.N. Husson. *Genes Dev* **2005**, *19*, 1692–1704.

[6] A. Singh, Y. Singh, R. Pine, L. Shi, R. Chandra, K. Drlica. *Tuberculosis* **2006**, *86*, 28–33.

[7] J.C. Betts, P.T. Lukey, L.C. Robb, R.A. MacAdam, K. Ducan. *Mol. Microbiol.* **2002**, *43*, 717–731.

[8] P. Fernandez, B. Saint-Joanis, N. Barilone, M. Jackson, B. Gicquel, S.T. Cole, P.M. Alzari. *J. Bacteriol.* **2006**, *188*, 7778–7784.

[9] V. Molle, L. Kremer. *Mol. Microbiol.* **2012**, *75*, 1064–1772.

[10] N.K. Singh, S.M. Selvam, P. Chakravarthy. *In Silico Biol.* **2008**, *6*, 485-493.

[11] A. Seal, P. Yogeeswari, D. Sriram, OSDD Consortium and J.D. Wild. *J. Cheminformatics* **2013**, *5*, 2–11.

[12] K.E.A. Lougheed, S.A. Osborne, B. Saxty, D. Whalley, T. Chapman, N. Bouloc, J. Chugh, T.J. Nott, D. Patel, V.L. Spivey, C.A. Kettleborough, J.S. Bryans, D.L. Taylor, S.J. Smerdon, R.S. Buxton. *Tuberculosis* **2011**, *91*, 277–286.

[13] T.A. Young, B. Delagoutte, J.A. Endrizzi, A.M. Falick, T. Alber. *Nat. Struct. Biol.* **2003**, *10*, 168-174.

[14] M. Ortiz-Lombardia, F. Pompeo, B. Boitel, P.M. Alzari. *J. Biol. Chem.* **2003**, *278*, 13094–13100.

[15] C.A. Lipinski, F. Lombardo, B.W. Dominy, P.J. Feeney. *Adv. Drug Deliv. Rev.* **2011**, *46*, 3–26.

[16] A. Wehenkel, P. Fernandez, M. Bellinzoni, V. Catherinot, N. Barilone, G. Labesse, M. Jackson, P.M. Alzari. *Febs Lett.* **2006**, *580*, 3018–3022.

[17] O. Korb, T. Stützle, T. Exner. *J. Chem. Inf. Model.* **2009**, *49*, 84–96.

[18] G.M. Morris, D.S. Goodsell, R.S. Halliday, R. Huey, W.E. Hart, R.K. Belew, A.J. Olson. *J. Comp. Chem.* **1998**, *19*, 1639–1662.

[19] G.L. Warren, C.W. Andrews, A.M. Capelli, B. Clarke, J. Lalonde, M.H. Lambert, M. Lindvall, N. Nevins, S.F. Semus, S. Senger, G. Tedesco, I.D. Wall, J.M. Woolven, C.E. Peishoff, M.S. Head. *J. Med. Chem.* **2006**, *49*, 5912–5931.

[20] F. Zuccotto, E. Ardini, E. Casale, M. Angiolini. *J. Med. Chem.* **2010**, *53*, 2681–2694.

[21] W.L. Jorgensen, E.M. Duffy. Bioorg. *Med. Chem. Lett.* **2000,** 10, 1155-1158.

[22] http://www.rcsb.org/pdb/home/home.do

[23] R. Powers, J. Copeland, K. Germer, K.A. Mercier, V. Ramanathan, P. Revesz *PROTEINS: Struct. Funct. Bioinformatics*, **2006,** 65,124-135.

[24] R. Powers, J. Copeland, J. Stark, A. Caprez, A. Guru, D. Swanson. *BMC Research Notes*, **2010, 4,**17-19.

[25] M.I. Davis, J.P. Hunt, S. Herrgard, P. Ciceri, L.M. Wodicka, G. Pallares, M. Hocker, D.K. Treiber, P. P Zarrinkar. *Nature Biothec.* **2011**, 29, 1046–1051.

[26] A.R. Katritzky, K. Akutagawa. *Tetrahedron Lett.* **1985**, *26*, 5935–5938.

[27] T. Ishiyama, M. Murata, N. Miyaura. *J. Org. Chem*. **1995**, *60*, 7508–7510.

[28] Villarino, R. Duran, A. Wehenkel, P. Fernandez, P. England, P. Brodin, S.T. Cole, U. Zimny-Arndt, P.R. Jungblut, C. Cerveñansky, P.M. Alzari, *J. Mol. Biol.* **2005**, *350*, 953–963.

[29] Molecular Operating Environment (MOE) version 2009.10; Chemical Computing Group Inc.: Montreal, Canada; http://www. chemcomp.com/.www.rcsb.org/pdb.

[30] D.A. Case, T.E. III Cheatham, T. Darden, H. Gohlke, R. Luo, K.M. Jr. Merz, A. Onufriev, C. Simmerling, B. Wang, R. Woods, *J. Comput. Chem.* **2005**, *26*, 1668–1688.

[31] K.L. Meagher, L.T. Redman, H.A. Carlson, *J. Comput. Chem*. **2003**, *24*, 1016–1026.

[32] J. Wang, W. Wang, P.A. Kollman, D.A. Case, *J. Mol. Graph. Model.* **2006**, *25*, 247–260.

[33] J. Wang, R.M. Wolf, J.W. Caldwell, P.A. Kollman, D.A. Case, *J. Comput. Chem.* **2004**, *25*, 1157–1174.

[34] AmberTools version 1.4; http://ambermd.org/#AmberTools.

[35] PyMOL version1.2r1; DeLano Scientific LLC: SanCarlos, CA http://www.pymol.org/.

Graphical abstract
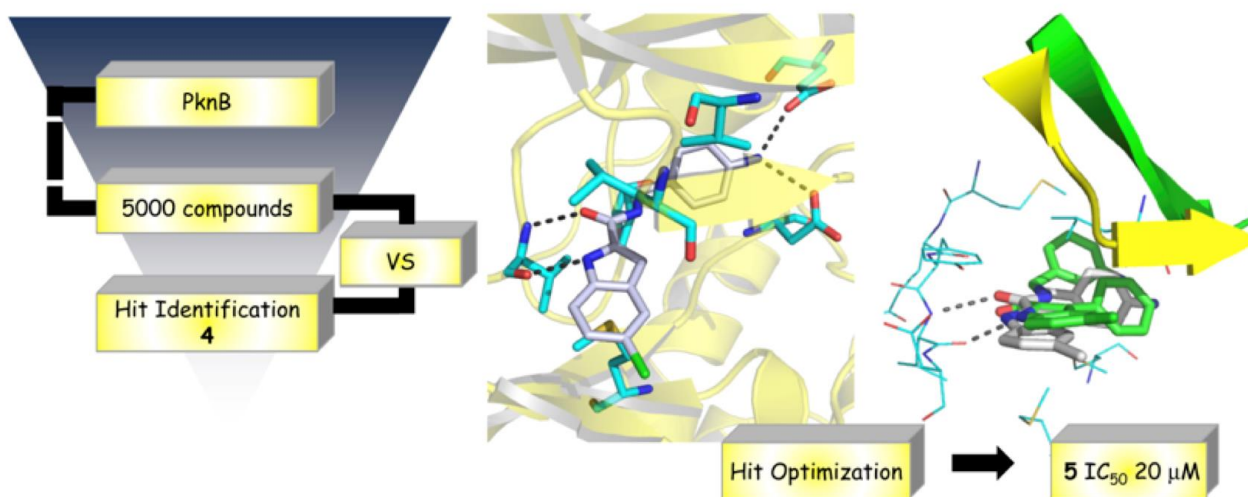
A structure-based virtual screening study into the ATP binding site of the Ser/Thr protein kinase PknB led to the discovery of compounds **1** and **2** as novel scaffolds endowed with PknB inhibition. A small compound library of compounds **3-9** was synthesized on the basis of the computational studies. N-(3-Aminobenzyl)-5-chloro-3-phenyl-1H-indole-2-carboxamide (**3**) showed promising inhibition of PknB with an IC_{50} value of 20 μM.